ThreeBond
TECHNICAL NEWS

Pressure-Resisting Mechanism of Reactive-Type Liquid Gaskets

<Part 1>

CONTENTS

Introduction

More than two decades have passed since liquid gaskets were applied to joints in various kinds of machines such as automobiles, construction machines, agricultural machines, ships, electrical appliances, and so on. All this while, the characteristics of liquid gaskets have constantly been improved, achieving great reliability as sealing materials.

Recently, the development of machines and robots for applying liquid gaskets on the assembly line has made rapid progress, and the so-called on-line gasket system (OLGS) has been adopted widely.

The OLGS is a total system to prevent leakage perfectly from flange surfaces through the combination of specially developed liquid gaskets and robots to apply the gaskets on assembly lines.

The adoption of the OLGS allows to reduce the cost extensively through the following steps:
(1) Reduction of gasket material cost,
(2) Use of light-weight, low-cost components,
(3) Saving in quantity of components and number of working processes,
(4) Reduction of working processes,
(5) Reduction of time for designing, and
(6) Rationalization of inventory management.

The liquid gaskets used in the OLGS are mostly made from silicone RTV or anaerobic acryl reactive compounds, which condense or polymerize after filling the mating surfaces to create an elastic adhesive layer for preventing leakage.

This is the first of two reports on the pressure-resisting mechanism of liquid gaskets.

1. Classification of Liquid Gaskets

Liquid gaskets currently commercially available are classified as in Table 1. Each of the products has its own merits for particular purposes and applying conditions, though the sealing characteristics of solidifying/solventless type, that is, reactive type, are distinctly different from those of non-reactive type gaskets, on the ground of the difference in the pressure-resisting mechanism.

The pressure-resisting mechanism of non-solidifying liquid gasket may be attributed to sealing by viscous nature of less fluidy liquid substance filling the gap between mating surfaces. When the gap grows, leakage may occur readily. The mechanism of leakage with non-solidifying liquid gasket can be explained by the theory of layer flow.

Table 1. Classification of Liquid Gaskets

		Non-solidifying	Solidifying
Non-solvent type		T B 1101 T B 1121	(Reactive) T B 1212 T B 1215 T B 1207B T B 1207C T B 1110B T B 1131
Solvent type	Organic solvent	*1 T B 1102 T B 1107	T B 1103 T B 1104 T B 1105 *2 T B 1201
	Aqueous		T B 1106 T B 1141

*1. TB1102 solidifies after a long time under particular application conditions.
*2. TB1201 is of silicone RTV solvent type.
(Note) TB stands for Three Bond.

While it is expected that liquid gasket of solidifying solvent type behaves in the same way as that of reactive type with respect to the pressure-resisting mechanism after the evaporation of solvent, the pressure resistance of the former is rather close to that of non-solidifying one, because the solvent evaporate so slowly as to have a long period of semi-solidified viscous state and the contraction on hardening is so much that the adhesive force is rather weak. For this reason, the application of solidifying liquid gasket is to be handled in the same way as non-solidifying one, and there is no clear theoretical treatment for this type of liquid gasket.

The reactive liquid gasket as silicone RTV and anaerobic acryl condenses or polymerizes after filling the joint to form an elastic adhesive layer on the mating surfaces for sealing. Accordingly, the gasket presents high pressure resistance at larger gaps between the mating surfaces. For the pressure exceeding the maximum joining pressure (2-2), the sealing is affected by the elasticity (elongation) of sealing agent.

2. Flange System

2-1 Elements of Flange System

Factors causing leakage at the bolt- fastened flange system involve finish precision, clearance and vibration during the operation. The most important factor for sealing is the mutual movement of the flange surfaces such as beating and shearing. Described below is each of the leakage factors.
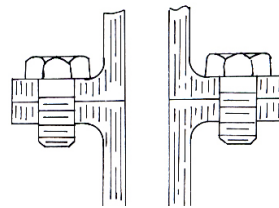

Fig. 1 Flange System

1) Finishing Accuracy

The maximum roughness on the ordinary flange surface is 10 ~ 20 μ or greater, and even that of precisely finished and polished flange surfaces is 0.1 μ (1000 Å).
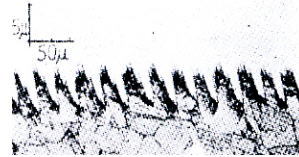

Fig. 2 Oblique Cut Section of Precision-lathed Copper Surface
The roughness is about 5 μ.

2) Inner Space (Micro-gaps between Metals)

When two flange surfaces of metal having good flatness are joined, it seems that the two surfaces contact with each other through the whole area. However, the area of actual contact is much less than the apparent contact area. For instance, when two steel surfaces of $20cm^2$ area each are joined and subjected to 1 ton load, the actual contact area is as small as $0.1cm^2$ (Table 2).
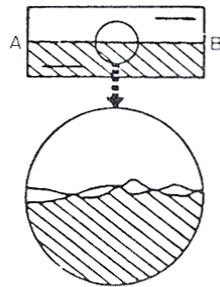
The actual contact area is much smaller than the apparent contact area AB.

Fig. 3 Metal Touch Contact

Table 2. Actual Contact Area

Surface Pressure kg/cm^2	Apparent contact area	Actual contact area
50		10 mm^2
25	20 cm^2	5 mm^2
5		1 mm^2
1		0.2 mm^2

* 0.1S, experiment with steel plates.

Even when the load is increased so that the plastic deformation occurs within the metal, the surface roughness persists. Accordingly, there exist inner spaces, even when flange surfaces having the finest finish precision and best flatness are joined together under high surface pressure.

At the joints in the ordinary machine components, the size of inner space is much greater than not only that of molecules of inner liquid but also its free volume.

3) Flatness

While the lathed flange surface has excellent flatness, the pressed sheet metal product has at times surface roughness greater than 100 μ.

4) Clearance

If one of two flange surfaces has poorer flatness, there occurs clearance. In some cases, clamping the joint with excessive force may cause a flange distortion, making clearance.

5) Bolts and External Factors

Generally speaking, in the flange system incorporating solid gaskets, sealing with the contact surface pressure requires clamping force by bolts. The initial clamping force is to be determined in consideration of stress relaxation of gaskets and loosening of bolts by external factors.

The flange system behaves in a very complicated manner owing to the external factors such as temperature, vibration, mechanical stress, and so on. For instance, in the case of automobiles, it is reported that there occur beating of 3 ~ 5 μ amplitude at the joint of cylinder head, and shearing more than 50 μ the joint of differential housing.

2-2 Maximum Joining Pressure

1) Three States of Flange System

When checking the behavior of the test flange system under fluid pressure, it is known that as the fluid pressure exceeds a certain critical value, called maximum joining pressure, which is determined by the pressure accepting area of the flange and the total clamping force of bolts, two mating surfaces fail to keep contact area and the flange system is fully opened (Fig. 4-3).
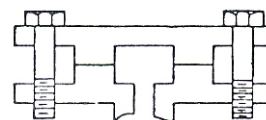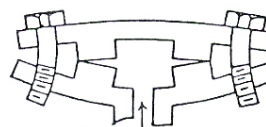

Fig. 4-1. P=0   (Joined state)

Fig. 4-2. 0<P≤Pℓ   (Quasi-open state)
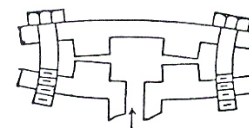

Fig. 4-3. P>Pℓ   (Full-open state)

Fig. 4 Three States of Test Flange

When the fluid pressure is null, the flange system is in the fully joined state (Fig. 4-1). As the fluid pressure is increased in short of the maximum joining pressure (Pℓ), the inside of joint surfaces opens, while the outside remains joined (Fig. 4-2).

2) Maximum Joining Pressured (Pℓ)

In a flange system shown in Fig. 5, with following denotations:

Upper cover flange:	: A
Lower main body flange	: B
Fluid pressure	: P (kg/cm^2)
Total clamping force of bolts	: Fb (kg)
Pressure accepting area	: Sp (cm^2)

The force joining A with B is Fb, and that lething them separate, that is, opening force is P (kg/cm^2) x Sp (cm^2). Hence, the joining condition in the flange system (Fig. 4-1, 2) is

$$Fb \geq P{\cdot}Sp \qquad (2.1)$$

The condition for full-opening (Fig. 4-3) is

$$Fb < P{\cdot}Sp \qquad (2.2)$$

The value of fluid pressure when the joining force is equal to the opening force, Fb = P·Sp, is called the maximum joining pressure of the flange system and represented by Pℓ. Therefore,

$$P\ell = Fb/Sp \qquad (2.3)$$

The maximum joining pressure is proportional to the total clamping force (joining force) and inversely proportional to the pressure-accepting area.
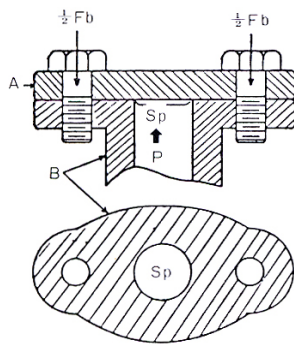

Fig. 5 Clamping Force and Pressure-accepting Area

When calculating the maximum joining pressure, the following three points are to be taken into consideration.

*1. When using a solid gasket, Fb must be equal to effective clamping force.

*2. When using a liquid gasket of which tensile strength and adhesive force are not negligible, the joining force should be set equal to Fb + tensile strength or adhesive force.

*3. When using a high-elastic liquid gasket, as Sp increases in the quasi-open state, the actual Pℓ decreases.

2-3 Measurement of Maximum Joining Pressure

Using a flange system illustrated in Fig.6, the opening of the joint at each step of pressurization was measured while increasing the fluid pressure gradually with the JIS·K 6820 Pressure Resistance Testing Machine. The test results reveale a linear relationship representing the flange distortion at the fluid pressure below Pℓ, and that the flange opening (elongation of bolts and gasket materials) is proportional to the fluid pressure above Pℓ.
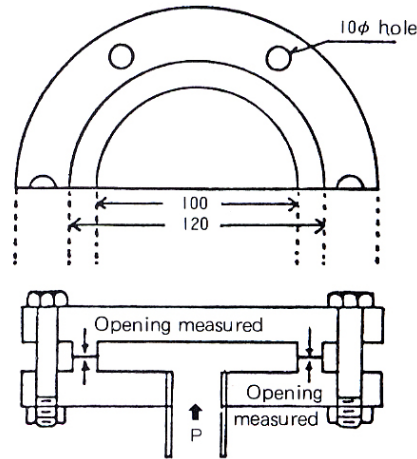
Bolts used: 3/8 inch × 6
Pressure accepting area: 78.5 cm^2

Fig. 6 Test Flange System

Fig. 7 shows the results obtained with 90kg-cm tightening torque for each bolt. Fb determined through the conventional means was 1,980kg, and the calculated value of Pℓ was 25.2kg/cm^2.

The measured value of Pℓ obtained graphically is 23.4kg/cm^2, which is slightly smaller than the theoretical value. This

discrepancy may be attributed to the factor mentioned in *3 of 2–2-2). The opening at the fluid pressure below $P\ell$ represents the quasi-open state, and varies depending upon the flange rigidity. The opening at the fluid pressure above $P\ell$ is proportional to the pressure.
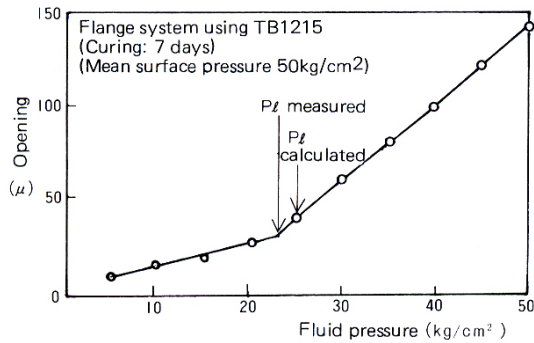

Flange system using TB1215
(Curing: 7 days)
(Mean surface pressure 50kg/cm^2)

Fig. 7 Measurement of Flange Opening

Fig. 8 shows the results for the cases with Fb=580kg (tightening torque 30kg-cm) and clearance=0.5. The calculated value of $P\ell$ was 7.4kg/cm^2, and the measured value obtained graphically was slightly smaller than the theoretical value for Three Bond 1215 (silicone RTV) and nearly equal to that for anaerobic A and anaerobic B.
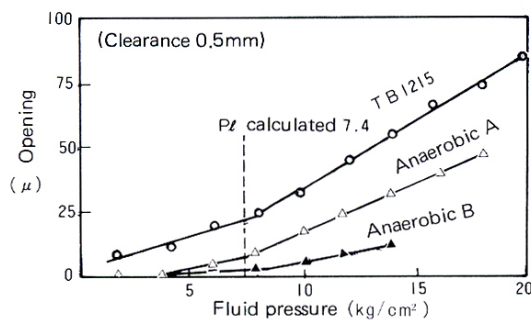

Fig. 8 Flange Opening for Different Liquid Gaskets

2-4 Factors Determining Sealing Properties of Flange System

The flange system consists of gaskets, flanges and bolts. The pressure accepting area of the flange and the clamping force of bolts determine the value of $P\ell$ which affects in its turn the sealing properties of the flange system. The initial height of the joint space (that is, the initial thickness of gasket layer) is determined by the finishing accuracy, flatness and clamping force of bolts.

The machining conditions of flange surface, flange shape and clamping force of bolts determine the value of $P\ell$ and the initial space of joint (initial shape of gasket layer) on the basis of respective mutual relationship. A block diagram showing the relationship is given in Fig. 9.
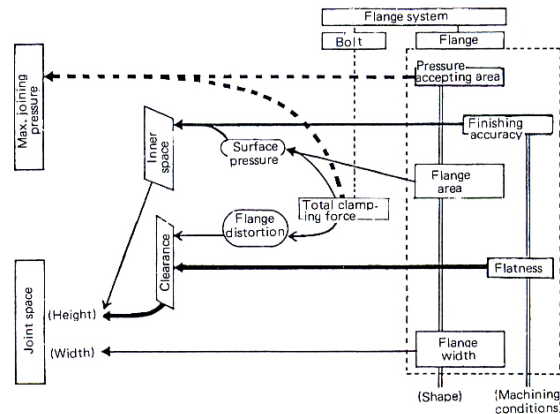

Fig. 9 Factors Determining the Sealing Property of Flange System

3. Pressure-Resistance Test

The basic pressure resistance test for the liquid gasket if generally carried out with circular test flanges by checking leakage while increasing the fluid pressure gradually. As the performance test, the leakage pressure test is conducted with elements of flange system changed.

This section will investigate the characteristics of reactive and non-solidifying luquid gaskets and the relationship between the pressure resistance test and the $P\ell$ value from the results of the pressure resistance test.

The test conditions accompany respective figures. For Figs. 10~12, flanges were joined together immediately after applying liquid gasket and allowed to cure for 7 days in the case of Three Bond 1215 (silicone RTV), and for 24 hours in the case of anaerobic sealant A, Three Bond 1102 and Three Bond 1121.

3-1 Characteristics of Reactive-Type and Non-Solidifying Type Liquid Gaskets

6

Fig. 10 shows the results of the pressure resistance test for various clearances. There appears great discrepancy between the curves for reactive and non-solidifying type liquid gaskets. In the case of non-solidifying type gasket, owing to the low cohesive force, the sealing property is readily lost in the presence of clearance, being thrusted away by the fluid pressure. On the other hand, in the case of reactive type liquid gasket, not only the increase of clearance but also the opening of flange at the fluid pressure exceeding $P\ell$ and covered by the adhesive force and elongation to prevent leakage.

Flange used: $100\phi - 116\phi$
Tightening torque: 30kg-cm
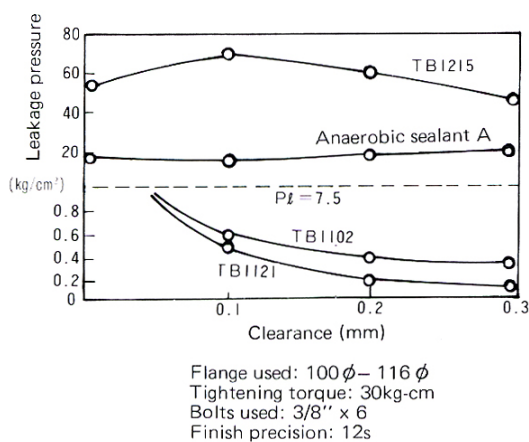Bolts used: 3/8″ × 6
Finish precision: 12s

Fig. 10 Clearance and Leakage Pressure

Fig. 11 shows the test results with the flange width changed.

Since the tightening force is held constant in order to eliminate the variation in $P\ell$ value, the surface pressure decreases as the flange width increases. Hence, the graph shows the relationship of pressure resistance to the simultaneous changes in flange pressure and surface pressure. In view of the fracture of gasket layer (4-3), this may be regarded as the cahnge in surface pressure under constant $P\ell$ value, rather than the change in flange width.

The results show that in the case of reactive type gasket, the lower the surface pressure is, the higher the sealing property becomes. This may be attributed to increased coverage for flange opening owing to the increase in the intitial thickness of gasket layer (inner space).
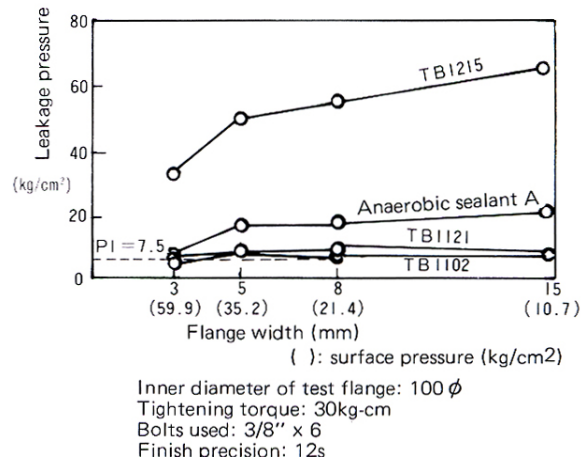

Fig. 11 Flange Width vs. Leakage Pressure

Fig. 12 shows the change in leakage pressure as a function of finish precision. It seems that the basically identical factor as in case of clearance shown in Fig. 10 is working.
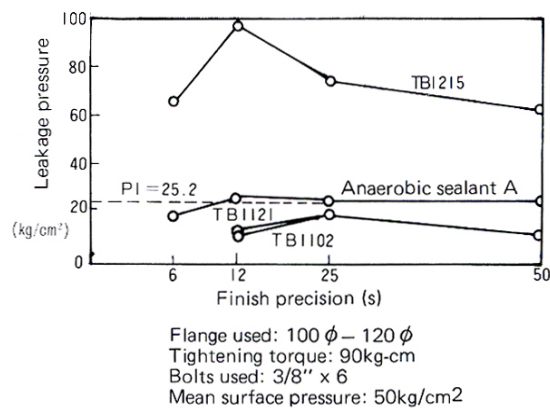

Flange used: $100\phi - 120\phi$
Tightening torque: 90kg-cm
Bolts used: 3/8″ × 6
Mean surface pressure: 50kg/cm2

Fig. 12 Finish Precision vs. Leakage Pressure

The points should be noted in Figs. 10~12 that as the height of the initial joint space (initial thickness of gasket) is reduced, the leakage pressure for four gaskets tends to be identical. This may be attributed to the face that when the initial thickness of gasket layer (inner space) is extremely thin, the vertical changes in various pressurizing stages exceed the difference in follow-up due to the adhesive or cohesive force of gasket, making the difference in gasket properties less pronounced.

3-2 Test Conditions and Maximum Joining Pressure

With a test falnge illustrated in Fig. 6, the test conditions determined by the flange

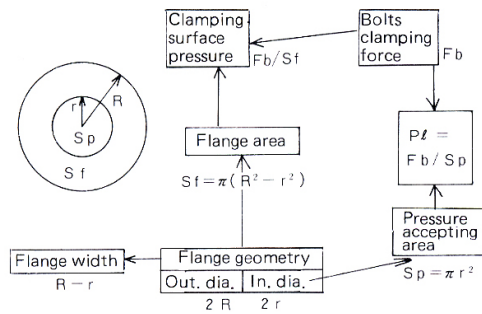geometry and bolt clamping force are related as shown in Fig. 13.

Fig. 13 Test Conditions and Pℓ Value

Since changing the test conditions often results in changes in Pℓ-value, the maximum joining pressure of the flange system must be taken into consideration when the characteristics of liquid gaskets are to be evaluated on the basis of the pressure resistance test results.
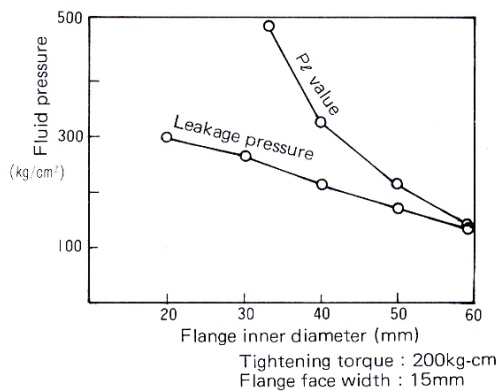

Tightening torque : 200kg-cm
Flange face width : 15mm

Fig. 14 Inner Diameter vs. Leakage Pressure

In the test shown in Fig. 14, the leakage pressure is plotted against the inner diameter of the flange. Since the flange face width if held constant, the flange area increases with the inner diameter. As the clamping force is constant, the clamping surface pressure and Pℓ-value decrease as the inner diameter increases.

In the test shown in Fig. 15, the inner diameter is increased while keeping the face width constant, as in case of Fig. 14, and the clamping force is increased as the flange area increases so as to keep the clamping surface pressure constant.

However, since the clamping force increases at a higher rate than the pressure accepting area, it is inevitable that the Pℓ value declines.

Mean surface pressure: 210kg/cm2
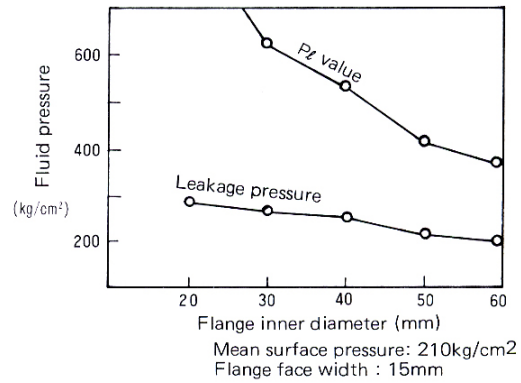Flange face width : 15mm

Fig. 15 Inner Diameter vs. Leakage Pressure

In the test shown in Fig. 16, the flange area is increased while the inner diameter is kept constant. As the clamping force is increased for keeping the clamping surface pressure constant, the Pℓ value increases.
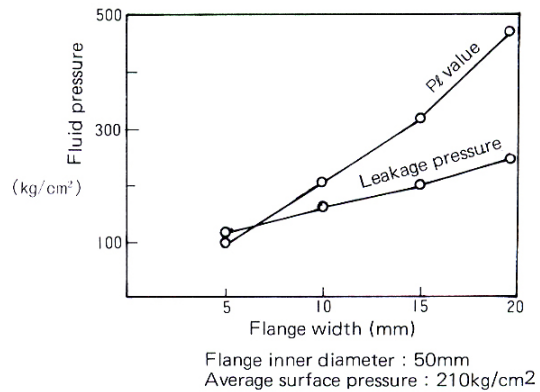

Flange inner diameter : 50mm
Average surface pressure : 210kg/cm2

Fig. 16 Flange Width vs. Leakage Pressure

In Fig. 17, where the flange geometry is unchanged, the Pℓ value rises with the clamping force.
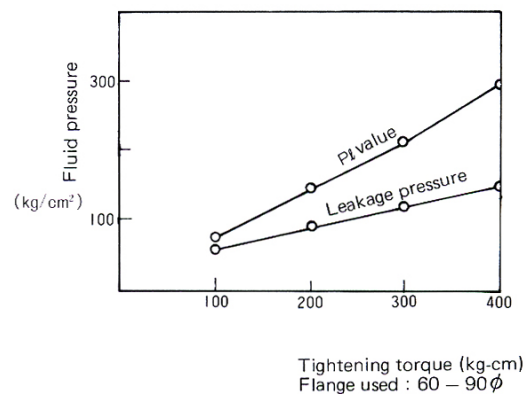

Tightening torque (kg-cm)
Flange used : 60 − 90 ϕ

Fig. 17 Tightening Torque vs. Leakage Pressure

In Fig. 18, where the clamping force and the inner diameter are held constant, the Pℓ value remains constant.
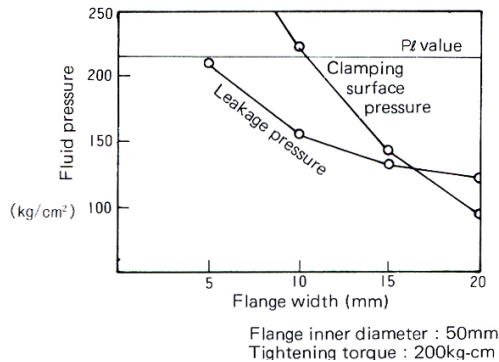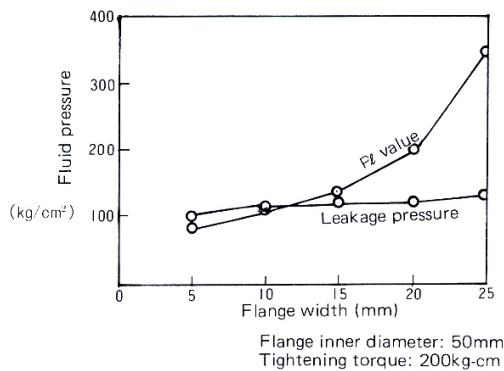

Fig. 18 Flange Width vs. Leakage Pressure

The decrease in clamping surface pressure and the increase in flange width associated with the increase in flange area are followed simultaneously.

In the test shown in Fig. 19, as the flange width is increased while keeping the outer diameter constant (with the inner diameter decreased), the Pℓ value rises in spite of fixed clamping force. The clamping surface pressure declines as the flange area increases.

In the pressure resistance tests illustrated in Figs. 14~19, non-solidifying solvent-type gaskets are used, of which sealing property is greatly affected by the longitudinal changes in the joint space at the time of pressurizing. Accordingly, the pressure resistance is directly related to the changes in the Pℓ value. When the Pℓ value is held constant (Fig.18), the clamping surface pressure to determine the initial thickness of gasket layer (inner space) is the main factor affecting the pressure resistance.

Fig. 19 Flange Width vs. Leakage Pressure

4. Pressure-Resisting Mechanism of Reactive-Type Liquid Gasket

4-1 Pressure-Resisting Mechanism of Non-Solidifying Liquid Gasket

The pressure-resisting mechanism of non-solidifying gasket is explained in terms of surface effect, close contact effect, thin layer effect and laminate flow theory.

1) Surface Effect

Also called anchor effect or hooking action. Due to the increase in the contact area between the liquid gasket and the joint face, as well as the improvement of wetting property, based on the surface roughness. This effect is also explained by the adhesion theory.

2) Close Contact Effect

This concerns wetting of liquid gasket. The theory of cohesion based on the surface tension and viscosity may be applicable.

3) Laminate Flows Theory

The behavior of non-solidifying liquid gasket at the joint may be explained by the formula given below, which is derived by applying Newton's law of viscosity to the laminate flow in a capillary tube:

$$Q = \frac{\pi R^4}{8\eta} \cdot \frac{P}{L} \quad (4.1)$$

Where   P: pressure difference across the tube,
         Q: volume of liquid flowing out in unit time,
         η: viscosity of liquid
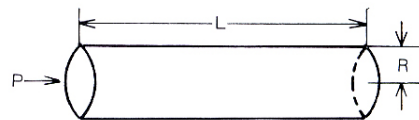   L: tube length
         R: tube radius

Fig.20 Laminate Flow in a Capillary Tube

This formula means that the volume of liquid Q flowing out of the tube in given time is proportional to the pressure difference across the tube P and the tube radius R, and inversely

proportional to the tube length L and the viscosity η. In order to have good pressure resistance, therefore, it is required that **1)** the inner pressure **(P)** is low, **2)** the flange width **(L)** is great and **3)** the distance between mating faces **(R)** is small.

Besides, the pressure-resisting mechanism of non-solidifying gasket can be explained by the theory of "steady flow of viscous fluid between two parallel planes" in the fluid dynamics.

4-2 Basic Theory of Reactive Liquid Gasket

When the fluid pressure is applied to the flange system including the reactive type liquid gasket, the gasket is subjected to the directly acting pressure P and the opening F which is determined by the relation of system conditions such as pressure accepting area, bolt strength and flange rigidity to the pressure P. The pressure resisting mechanism of gasket layer is explained by the relationship of resultant force of F and P, adhering force between gasket layer and flange face, and cohesive force of gasket materials.

When F and P act, the gasket layer behaves elastically to keep sealing.

1) Hooke's Law

The Hooke's law states that strain is proportional to external force (stress) within the range of elastic deformation. This relation covers elongation, compression, shear and torsion. Generally, it is represented by the formula given below.

External Force (stress)
= Elastic Modulus x Strain (4-2)

This formula applies to every kind of external force (stress)-strain relationship.

2) Property-Dependent Difference in Elastic Modulus

It is evident that the elasticity of rubber is markedly different from that of metal, with respect to Young's modulus (E) or Poisson's ratio (σ). For metal, $E = 10^{11} \sim 10^{12}$ dyn/cm^2, while for rubber $E = 10^{6} \sim 10^{7}$ dyn/cm^2. The range of reversible elasticity, where the Hooke's law applies, is 1% or less for metal, but 200% or more for rubber.

Table 3. Elastic Modulus

Substance	E (dyn·cm^2)	σ	K (dyn·cm^2)	n (dyn·cm^2)
Iron	20×10^{11}	0.25 ~ 0.33	18×10^{11}	7.9~89×10^{11}
Copper	13　"	0.26 ~ 0.34	14　"	3.9 ~ 4.6×"
Nickel	20　"	0.31	18　"	7.7　"
Lead	1.6　"	0.45	5　"	0.56　"
Elastic rubber	15~50×10^7	0.46~0.49	–	5 ~15×10^6

E···Young's modulus　　σ······ Poisson's ratio

K······shearing elastic modulus　　n······volume elastic modulus

4-3 Fracture Mechanism of Reactive Liquid Gasket Layer

In a flange system with horizontal joint face, the external force to the gasket layer can be decomposed to horizontal direct force of fluid pressure P and vertical opening force (indirect force of fluid pressure). P and F are converted to inner stresses p and f, respectively, of different magnitude and direction through the elastic deformation of gasket layer. When the resultant force of p and f exceeds the cohesive force of gasket Fs or adhering force Fa, the fracture of the gasket layer starts.

1) Deformation and Inner Stress due to Fluid Pressure

When the gasket layer is subjected to fluid pressure P, if the length of layer (flange width) L is sufficiently long in comparison to the thickness of layer h, its deformation may be represented as shown in Fig. 21. (In Fig. 21, AY represents vertical section and BX horizontal section.)
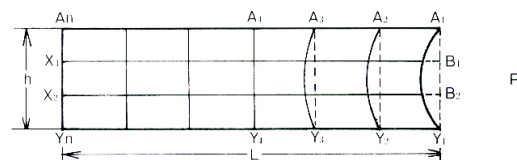
The deformation of various parts of inner layer shown in Fig. 21 (layer between B_1X_1 and B_2X_2) is considered in Fig. 22. The inner stresses for three parts are given by:

for Fig. 22-1, $\quad p_1 = E \dfrac{\Delta l_1}{l}$ (4.3)

for Fig. 22-2, $\quad p_2 = E \dfrac{\Delta l_2}{l}$ (4.4)

for Fig. 22-3, $\quad p_3 = E \dfrac{\Delta l_3}{l}$ (4.5)

where E: Young's modulus of gasket

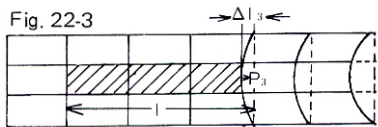Since $\Delta l_1 > \Delta l_2 > \Delta l_3$, it may be concluded that $p_1 > p_2 > p_3$ and $p_1 = P$, $p_{4\text{-}n} \doteqdot 0$.
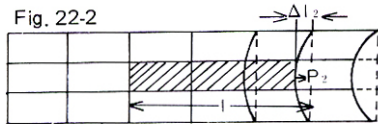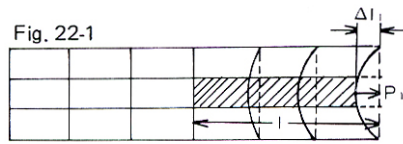
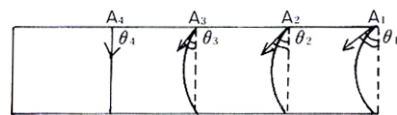

Fig.22 Inner Stress due to P

Fig.23 Stress at Interface

For the deformation at the interface, shearing elastic modulus is applied, and the inner stresses at $A_1 \sim A_4$ in Fig. 23 are given by

$$
\left.
\begin{aligned}
p_{A1} &= n\theta_1 \\
p_{A2} &= n\theta_2 \\
p_{A3} &= n\theta_3 \\
p_{A4} &= n\theta_4 = 0
\end{aligned}
\right\} \quad (4.6)
$$

Where   n: shearing elastic modulus of gasket

Since $\theta_1 > \theta_2 > \theta_3 > \theta_4$, it may be concluded that $p_{A1} > p_{A2} > p_{A3} > p_{A4}$.

From these discussions, it is evident that the inner stress due to P is greates at the contact face with liquid (plane A_1Y_1 in Fig. 21).

2) Deformation and Inner Stress due to Opening Force

In Fig. 24, it is assumed that the area of mating face (adhering area between gasket and joint) S_1 is given by the following formula when the thickness of gasket layer becomes from h to h+Δh under the action of opening force F.

$$F / S_1 = E \frac{\Delta h}{h} \qquad (4.7)$$

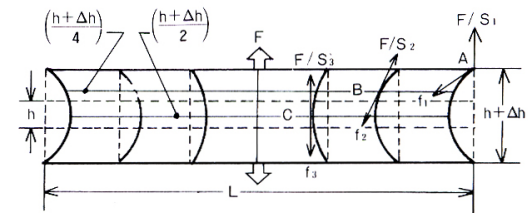Where   E: Young's modulus of gasket

Fig.24 Deformation and Inner Stress due to F

Sections in the vertical direction are deformed at different curvatures. (The plane L/2 at the middle of joint face is deformed in the vertical direction only.) F/S is equilibriated with the inner stress f of gasket in the tangential direction of each section.

In Fig. 24, if the areas of gasket layer sections in parallel to the joint face, ¼ (h+Δh) and ½ (h+Δh) are S_2 and S_3, respectively, the inner stress f in these sections and joint face are given by

$$
\left.
\begin{aligned}
&\text{[Joint face]} \quad f_1 = F / S_1 \\
&[\tfrac{1}{4}(\text{h}+\Delta\text{h}) \text{ section}]\ f_2 = F / S_2 \\
&[\tfrac{1}{2}(\text{h}+\Delta\text{h}) \text{ section}]\ f_3 = F / S_3
\end{aligned}
\right\} \quad (4.8)
$$

Since $S_1 > S_2 > S_3$, $f_1 < f_2 < f_3$, and the tensile stress f in the gasket layer due to the opening force F is greatest at the ½ (h+Δh) section. (The stress acting to each section as a whole is uniform and equal to F.)

3) Fracture Equation

Since the stress in the gasket layer due to P is greatest at the A_1Y_1 plane in Fig. 21 and the stress due to F is greatest at the ½ (h+Δh) section in Fig. 24, the interface fracture in the gasket layer starts from A or A', and the cohesion fracture occurs at B (Fig. 5).
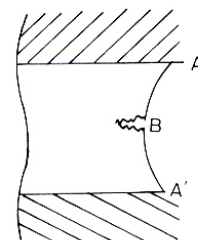

Fig.25 Fracture of Gasket Layer

The fracture force due to opening force F and fluid pressure P may be decomposed in the directions of X-axis (horizontal) and Y-axis (vertical).

In Fig. 26, under the opening force F, inner stress f_1 and f_2 occur at points A and B, respectively, in the tangential directions to the curve AB of gasket layer. Decomposing f_1, one obtains at point A,

$$\left.\begin{array}{l} X_A = f_1 \sin\theta \\ Y_A = f_1 \cos\theta \end{array}\right\} \quad (4.9)$$

and at point B,

$$\left.\begin{array}{l} X_B = 0 \\ Y_B = f_2 \end{array}\right\} \quad (4.10)$$
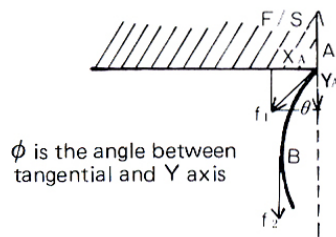

ϕ is the angle between tangential and Y axis

Fig. 26 Decomposition of f

In Fig. 27, the fluid pressure acts in the normal direction of the curve AB, and its Y-component (Y_A) at point A is non-fracture force. When decomposing P, at point A,

$$\left.\begin{array}{l} X_A = P \sin\left(\dfrac{\pi}{2} - \theta\right) = P\cos\theta \\[2mm] Y_A = -P\cos\left(\dfrac{\pi}{2} - \theta\right) = -P\sin\theta \end{array}\right\} \quad (4.11)$$

at point B,

$$\left.\begin{array}{l} X_B = P \\ Y_B = 0 \end{array}\right\} \quad (4.12)$$

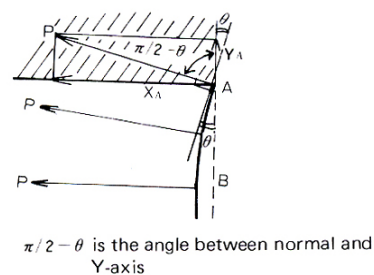$\pi/2 - \theta$ is the angle between normal and Y-axis

Fig. 27 Decomposition of P

Since the interface fracture occurs under the resultant force at point A, that is, the sum of equations (4.9) and (4.11), the condition for interface fracture may be written as

$$f_1 (\sin\theta+\cos\theta) + P (\cos\theta-\sin\theta) > Fa \qquad (4.13)$$

or

$$\underbrace{f_1\sin\theta + P\cos\theta}_{\substack{\text{X-component} \\ \text{(shearing stress)}}} + \underbrace{f_1\cos\theta - P\sin\theta}_{\substack{\text{Y-component} \\ \text{(tensile stress)}}} > Fa \qquad (4.14)$$

Where Fa: adhering force of gasket

On the other hand, as the cohesion fracture occurs under the resultant force at point B, that is, the sum of equations (4.10) and (4.12), the condition for cohesion fracture may be written as

$$f_2 + P > Fs \qquad (4.15)$$

Where Fs is cohesive force of gasket.

5. Pressure-Resistance Test and Fracture Equation

5-1 Properties of Reactive-Type Gaskets

The properties and adhesive strength of hardened reactive-type liquid gaskets such as anaerobic acryl (flexible type) and silicone RTV (Three Bond 1215 for liquid gasket and low modulus type) are shown in Table 4 and Figs. 28 and 29, respectively.

Table 4. Properties of Hardened Liquid Gaskets

| Gaskets / Item	A *	B	C	TB1215
	Anaerobic acry1 {flexible type}		Silicone RTC {low modulus}	Silicone RTV
Coefficient of linear contraction (%)	3		0.3	
Hardness (JIS·A)	90	90	10	45
Tensile Strength (kg/cm²) — 150% modulus	-	-	1.5	5.3
Tensile Strength (kg/cm²) — At fracture	105	-	10	10
Elongation (%)	37	30	1500	400
Peeling adhesive strength (kg/25mm)	0.8	0.6	0.9	2.0
Shearing adhesive strength	Fig. 28			
Tensile adhesive strength	Fig. 29			

∗ Equivalent to Three Bond 1131
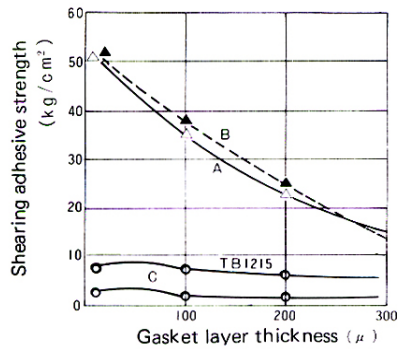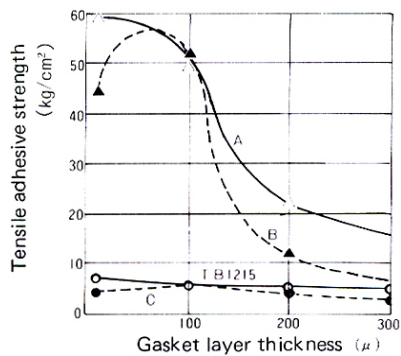
Fig. 28 Shearing Adhesive Strength

Fig. 29 Tensile Adhesive Strength

5-2 Gasket Properties and Fracture Equation

1) Application to Interface Fracture Equation

With regard to f_1, form equations (4.7) and (4.8),

f_1 = E x Elongation of gasket (flange opening) /Initial thickness of gasket (initial height of joint)   (4.16)

where E is determined on the basis of relationship between the elongation and the tensile strength within the range of elastic deformation of gasket.

As for Fa, adhesive force of gasket layer to flange face, strictly speaking, the adhesive force is the binding force between adhesive molecules and joint molecules, which can not be determined by the measurement. The adhesive strength is equal to the fracture strength of the actual joint, and is affected by adhering force, cohesive force of adhesive and fracture conditions, excepting for cases where the joint itself is broken.

Since the true adhesive force between the flange face and the gasket layer can not be determined, the tensile adhesive strength is used as an approximation.

The value of θ which is determined by the geometry of gasket layer, its change and fluid pressure and can be measured experimentally, is estimated here on the basis of hardness and elongation.

2) Application to Cohesive Fracture Equation (4.15)

The cohesive force Fs which is the intermolecular binding force of gasket may be estimated on the basis of tensile strength and compressive strength. In view of the decomposition of inner stress (Figs. 26 and 27); however, it may be regarded that the tensile strength corresponds to f and the compressive strength to P. Moreover, most of P at point B in Fig. 27 seems to be reduced by the compressive stress of gasket layer. So, the equation (4.15) may be approximated by

$$f > Fs\ (f)   (4.17)$$

where Fs (f) is the tensile strength of gasket at fracture.

From the equation (4.8), f_1 at the interface is different from f_3 at the $\frac{1}{2}(h+\Delta h)$ face. Since in the actual joint the length of gasket layer (flange width) is adequately great in comparison to the gasket thickness h, the difference between S_1 and S_3 in (4.8) may be ignored. Hence, f in (4.17) may be regarded to be equal to f_1 in (4.16).

5-3 Theoretical and Experimental Values

In the pressure resistance test using Three Bond 1215 and anaerobic sealant A, the experimental values are compared with the theoretical ones (under the same test conditions as shown in Fig. 8, except for clearance = 0.1mm).

1) Calculation of Theoretical Value

From (4.13) and (4.16),

$$E\ \frac{\Delta h}{h}\ (\sin\theta + \cos\theta) + P\ (\cos\theta - \sin\theta) > Fa   (4.18)$$

and from (4.17),

$$E\ \frac{\Delta h}{h}\ > Fs\ (f)   (4.19)$$

These relations are used for calculating the theoretical values. The calculation of each term and the theoretical value of maximum resisting pressure (fracture pressure) are shown in Table 5. (The value of θ is estimated to be within the range shown in the table.)

Table 5. Calculation of Theoretical Values

Item	Remarks	TB1215		Anaerobic A	
E (kg/cm²)	**TB1215: the 150% modulus value in Tab 5 is put into (4.16).** Anaerobic sealant A: determined from the opening difference between TB1215 and anaerobic sealant A in Fig. 8.	3.533		43.57	
Δh (μ)	Since the elongation of gasket layer Δh (opening length) at fluid pressure exceeding Pℓ is proportional to the pressure P, it is assumed that Δh=kp and k is determined from Fig. 8. (For the pressure below pℓ.. Δh=0.)	Δh=5(P - Pℓ) =5p - 37.50		Δh=4.25(P-Pℓ) =4.25p-31.0	
h (μ)	From the condition.	100		100	
$E\frac{\Delta h}{h}$ (kg/cm²)		0.176p-1.32		1.85p-13.89	
Fa (kg/cm²)	Tensile adhesive strength at film thickness 100 μ in Fig. 29.	5.6		50	
Fs (kg/cm²)	Tensile strength in Table 4 (at fracture)	10		105	
θ	TB1215: 45°~50° A: 20°~30°	45°	50°	20°	30°
	sinθ+cosθ	1.414	1.409	1.2817	1.3660
	Cosθ-sinθ	0	0.123	0.5977	0.3660
Max. resisting pressure (kg/cm²)	Interface fracture	29.90	59.26	22.82	23.82
	Cohesive fracture	64.09		64.19	

2) Theoretical and Experimental Values

The results given in Table 5 are compared with the results of the pressure resistance tests.

Theoretical values:
TB1215: 29.90 ~ 59.26kg/cm²
Anaerobic sealant A:
   22.82 ~ 23.82kg/cm²

Measured values:
TB1215: 39kg/cm²
   (extrusion eliminated)
Anaerobic sealant A: 20kg/cm²

Two sets of values are nearly coincident with each other.

While it is difficult to decide experimentally whether the fracture is interface or cohesive, the results of the theoretical calculation suggests the interface fracture.

3) Merits of Pressure Resistance Based on Gasket Properties

While TB1215 presents high pressure resistance owing to the elastic effect, the pressure
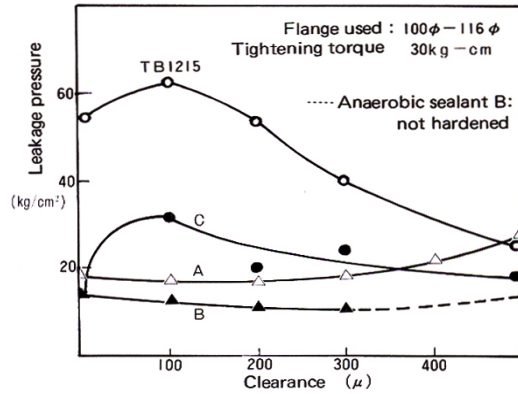
Fig. 30 Clearance vs. Leakage Pressure

resistance varies extensively depending upon the magnitude of θ. In case of Table 5, if θ is changed from 45° to 50°, the maximum resisting pressure is doubled from 30kg/cm² to 60kg/cm².
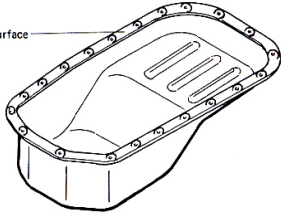
In the experiment with TB1215, the pressure resistance declines when the clearance is increased (with θ reduced). This coincides with the trend seen in the results of the theoretical calculation. The larger fluctuation in the high-elastic gasket materials as encountered in many pressure resistance tests may be attributed to changes in θ due to protrusion or other uncertain factors.

The anaerobic sealant A is gasket material of relatively low elasticity, and its pressure resistance is acceptable for the practical purpose. The pressure resistance is not affected so extensively by the change in θ, and the results are fairly constant. This can be demonstrated both theoretically (Table) and experimentally (Figs. 10, 12 and 30).

As for the adhesive force required for the gasket material, which often comes to question, it is evident from the theoretical fracture equation, that greater adhesive force is required, in case of lower-elastic materials, when f is determined by Δh/h (opening ratio). In case of actual bolt-clamped flanges, the main factor of fracture is f based on the opening (Δh).

It should be noted with regard to the elasticity of gasket materials that the apparent elasticity is much affected by the rate of fracture (deformation). For instance, if the opening proceeds quickly, the gasket material behaves as hard one, and if very slowly, as soft material. This is the problem of rheology. It seems that the practical study is much more important than the theoretical one.

Comparison of OLGs with Solid Gaskets

#	Item	Remarks
1	Type of Industry	Automobile
2	Applicable Machine & Parts	Oil pan (passenger car: 2,000cc)
3	Production Quantity	10 thousand units per month
4	Measurement, Surface Area and Weight	22cm × 48cm × 170cm, 2.5kg, Peripheral length of oil pan: 130cm, Surface width: 20mm
5	Material	Cold pressing (rolled steel SPC3)
6	Product Name and Grade	Three Bond 1212D / Conventional product: Rubber cork
7	Quantity of Consumption	13g/unit / 1 sheet/unit
8	Product Price	6,000 yen/kg / 350 yen/sheet
9	Amount of Consumption	6 yen/g, 78 yen/unit / 350 yen/unit
10	Production Quantity and Total Consumption	130kg / 10 thousand sheets
11	Total Amount	780 thousand yen / 3.5 million yen
12	Price of Device and Parts	880 yen/piece / 880 yen/piece
13	Purpose and Contents	Increase in sealing property and cost reduction

#	Item	Remarks
14	Application Conditions	Engine oil scattering. Temp: 120°C max. Inner pressure: 0.5 kg/cm^2 max. Acceleration of vibration: 4G max. Clamping pressure: 30 kg/cm^2
15	Problem and Countermeasure	Since solid gaskets generate permanent distortion over a long period of use, silicone type liquid gaskets will be used hereafter.
16	Failure	No problem. Complete sealing. Three Bond 1207C is superior in decomposition.
17	Reason and Cause of Adoption	Cost reduction is possible.
18	Schematic drawing	Applied surface

		Evaluation of Function			Evaluation of Profit and Loss				
	Item	Three Bond Product	Conventional product	Reason	Explanation	Loss	Three Bond product	Conventional product	Detailed Explanation of Profit and Loss Evaluation
Material cost	1. Material cost and working cost 1-1 Material cost 1-2 Auxiliary material cost 1-3 Working cost	◎	×	Price difference	1-1 Material cost (gasket) 1-2 Reduction in number of clamping bolts 1-3 Simplification of flange surface finishing work	Cost	78 yen 54 yen	350 yen 66 yen 290 yen	O Number of bolts (MB) 22→18 @ 3 yen/bolt O Reduction in oil pan working cost O Pressure ridges also can be omitted. (Strengthening of the designated surface……No throttling and bending work)
Outline	2. Instruction manual, display and design 3. Service (URC, technique)	O	O						Reduction of approx 30% of 880 yen→290 yen

Handling	4. Stock control (inclusive of outside products)
	4-1 Ordering stock cost
	4-2 Storing condition and period
		O	Δ	Labor cost	No stock control of gaskets classified for every kind of car	Time	17 yen	18 yen	O In case of OLG, a half man/month is reduced.
									  Labor cost: 30 yen/min, 1,800 yen/hour,
									  14,400 yen/day, 360,000 yen /month
									  180,000 ÷ 10,000=18 yen

Handling	5. Working property
	5-1 Equipment, tool and condition
	5-2 Time
	5-3 Operational property (mechanical skill)
	5-4 Worker's incentive
		O	Δ	Labor cost	5-1 Use of application robot
					5-2 No mechanical skill (No educational training: 10% reduction of labor cost)
					5-3 No labor dispersion (increase in working will: 3 times labor cost)
						Time		5 yen
								0.50 yen
								
								2.50 yen
									O Cost of robot: 10 million yen/unit, 170 thousand yen/month at amortization for 5 years
									  170,000 yen per unit ÷ 10,000 = 17 yen
									O Setting of solid gaskets 5 yen/10 sec
									  Labor cost: @ 30 yen/min, @ 0.50 yen/sec,
									  Setting time: 10 sec

Major Characteristics	6. Process control (doubling)	◎	×	Labor cost	No inspectional defect	Percent inspection defective		4.10 yen
								{1% 100 units}
									O Decomposition time: 30 sec
									O Gasket replacement
									  350 yen × 100 units=(35,000 yen/10,000 units)
									  =3.50 yen
									O Bolt clamping: 30 sec, Reinspection: 1 min
									  60 yen × 2 min × 100 units = 6,000 yen ÷ 10,000 units = 0.60 yen
									  3.5 yen+0.60 yen = 4.10 yen
									O A defective car detected (completed car) requires 2 hours for repair.
									  Security cost: 10,000 yen/unit
									  3,600 yen (for 2 hours) × 100 units = 360,000 yen ÷ 10,000 units = 36 yen
									  10,000 yen × 100 units ÷ 10,000 units=100 yen
									  36 yen + 100 yen = 136 yen

Major Characteristics	7. Sealing efficiency 7-1 Sealing effect (prevention of trouble caused by leakage) O Pressure resistance O Airtight property O Volumetric shrinkage O Heat resistance cycle changed with time 7-2 Chemical resistance O Water, oil, gas and chemicals O Existence of base metal damage	◎	Δ	Material cost Labor cost Security cost	Complete oil-tight sealing with use of OLG When solid gaskets are used for a long time, permanent distortion is produced, generating oil leakage	Device in use Percent defective		136 yen {1% 100 units}	
Disadvantage	8. Reliability & Safety	◎	Δ					d	
Disadvantage	9. Recycle	×	Δ						
Disadvantage	10. Model change (Design change)	◎ ×			OLG can be used as it is even if the design of machines or parts is changed.			d	
					Total		145 yen	872.10 yen	

Total Cost Reduction

1 unit	727,10 yen+α
1 month	7,271,000 yen+α
1 year	87,252,000 yen+α

List of Applying Robots and Machines

Following types of robots and machines for applying reactive liquid gasket are available.

For further details, please request the catalogue.

Applying Method	Models	Principle of Operation	Outline and Main Features
Tracing	TRT-22 TRT-23 TRT-26	Template	With an iron plate of same geometry as the pattern to be applied as a guide, a magnet roller equipped with a delivery nozzle is driven to trace. Characterized by small size, low cost and maintenability.
	TRO-92	Photo cell	Line drawing for the pattern to be applied drawn on white paper is read by a photo cell and traced by the nozzle driven by a servo motor. Characterized by small size, low cost and pattern interchangeability.
	TRC-60	Computer	Coordinate values of line drawing for the pattern to be applied are stored in a paper tape through a puncher. The punched tape is input to a computer to trace by driving the delivery nozzle on an orthogonal table through a servo motor. Characterized by high accuracy and pattern interchangeability.
	TRC-65		The pattern to be applied is input to the computer through the keyboard on a teaching box while moving the delivery nozzle manually along the pattern. The nozzle is driven by an orthogonal table through a servo motor to trace. Characterized by high speed, easy inputting and pattern interchangeability.
	TRC-70		The methods of inputting and tracing are same as those in TRC-65. Three-dimensional application available. Owing to the linear operation simultaneously on three axes, the nozzle can trace an oblique line in three-dimensional space or an circular arc in a plane defined by any two of three axes. Characterized by high speed, easy inputting and pattern inter-changeability.

TRT-26

TRO-92

TRC-70
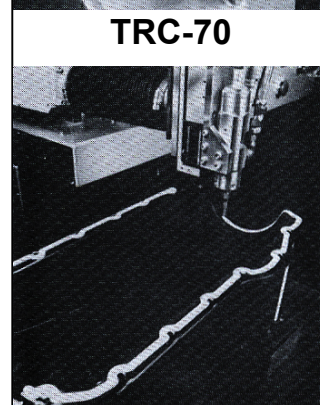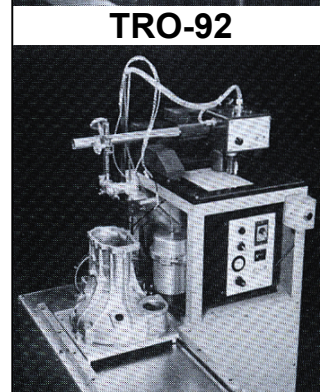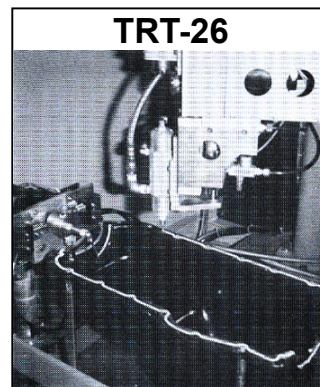
Contents of

Pressure-Resisting Mechanism of Reactive Type Liquid Gaskets

(Part 2)

to appear on the next issue